Summer Students Project
Dynamic Light Scattering of Colloidal Solutions near the Glass Transition

Nina A. Sapoletova (Moscow State University)
Sebastian Szillat (Universität Wuppertal)

Supervisor: Christian Gutt

14.09.2007

Contents

1 Scattering theory **4**
1.1 Colloidal solutions 4
1.2 Scattering in general 5
1.3 Formalism 5
1.4 Intensity and Scattering Pattern 6
1.4.1 Formfactor 6
1.4.2 Structure factor 7
1.5 Photon correlation spectroscopy (PCS) in colloidal dispersions . 8
1.6 Temperature dependence of viscosity 10

2 Experiment **11**
2.1 Experimental setup 11
2.2 Viscosity correction 11
2.3 Temperature correction 12

3 PMMA **13**
3.1 PMMA diluted sample 13
3.1.1 Autocorrelation function 13
3.1.2 Diffusion constant 13
3.1.3 Determination of radius 14
3.1.4 Intensity and Form factor 15
3.2 PMMA concentrated sample 15
3.2.1 Intensity 15
3.2.2 Static structure factor 15
3.2.3 Hydrodynamic interactions 17

4 pNIPA - in 3 concentrations **18**
4.1 Static Analysis 18
4.2 Particle radius 19
4.3 Discussion of dynamic behavior (1) 20
4.4 Discussion of dynamic behavior (2) 21
4.5 Discussion of dynamic behavior (3) 21

5 Conclusion **27**

Abstract

Dynamic light scattering (DLS) is one of the most popular methods for studying colloidal suspensions. This method allows measuring the size of particles, the viscosity or many other characteristics of colloidal solutions (static factor, hydrodynamic functions).

In this work we investigate by means of DLS the dynamic and static behavior of PMMA (poly methyl metacrylate) and Poly-NIPA (poly N-isopropyl-acryl amid) aqua solutions with different volume fractions. We also study the properties of thermo sensitive Poly-NIPA particles.

1 Scattering theory

1.1 Colloidal solutions

A colloidal solution consists out of particles with sizes between 1 and 1000 nm, that are solved in a proper solvent. In our experiment we use the polymers PMMA (poly methyl metacrylate) and Poly-NIPA (poly N-isopropyl-acryl amid) in a aqueous dispersion.

PMMA

PMMA is produced by polymerization of the monomer methyl methacrylat. During this process different parameters can be tuned to determine the length of the chains. By using crosslinking molecules these chains create a network. Due to the polymerization in emulsion and the hydrophobic character of the PMMA-polymer-backbone these molecules form a shape that is pretty much a sphere, in order to minimize the surface that is in contact with water. Ionized sulfate-groups are connected to the surface and due to this "surface-charges" the whole molecule acts like a big ion, interacting with his neighbor atoms.

polyNIPA

Is similar to PMMA. It's build up out of the the monomers isopropylachrylamid which are connected in a radically polymerization. It's crosslinked by N-methylenbisacrylamid and forms spheres of predictable sizes with charged surfaces.

The very special feature about pNIPA is the change of the spheres size with temperature. pNIPA is a thermosensitive polymeric material and accordingly it has a transition temperature, in our case at 30° and 35°C in aqueous solutions. Below this temperature the pNIPA absorbs a lot of water in its network and thus the effective radius of the particles grows. For higher temperatures the particles show a more or less constant radius. This process of growing and shrinking is reversible. In a lucky combination of particle-size and concentration it is possible to reach a liquid-glass phase transition in a moderate temperature-range of 10° to 30° C.

Glass transition

The theory that describes the dynamic behavior of colloidal particles in high diluted systems is sophisticated and makes good predictions for our experiments. For the glassy-phase however there is no such fully developed theory available. The glass transition temperature is the temperature below which the physical properties of the system vary in a manner, similar to those of a solid phase (glassy phase) and above which the system behaves like a liquid. In easy words one can describe the glassy phase of a colloidal system as a phase in that the particle feel each other, respective the interactions between them start to have

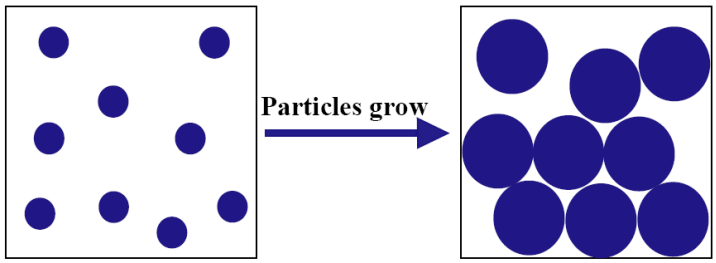

Figure 1: Liquid and glassy phase

influence on the single particles behavior. There are two commonly known ways to reach a glass transition in a colloidal system.

- One method is to concentrate a sample, by what you have more particles per volume and consequently smaller distances between the particles, resulting in stronger interactions.
- The more comfortable method requires very special systems, for example thermo sensitive polymeers, such as the pNIPA-particles - dispersed in water, as we are using. By tuning the temperature we can change the individual particles size. Thus the mean distance between the particles effectively shrinks. When the particles start to feel their neighbors they try to arrange in a mode of minimal energy (see figure 1). This can cause very regularly, crystal like structures with the according scattering-behavior.

1.2 Scattering in general

When a visible photon (laserbeam) hits a target it's electrons are accelerated by the electrical field of the EM-wave. As long as we are dealing with photon-energies $\ll$ binding-Energy (true for visible light) the accelerated electron works as a hertz'dipole and emits a secondary wave with the same wavelength as the stimulating primary-wave. (works for weakly bound that means weakly damped electrons as for example valence-electrons). As we are analyzing samples with more than one electron the secondary waves interfere, resulting in a scattering pattern.

In scattering you are sensitive to structures with a size that is in the same regime as the used wavelength. That means for a optical laser you can analyse electon-density differences (structures) in the nm regime, as for example caused by colloidals solved in a solvent.

1.3 Formalism

In a scattering experiment the incoming beam is scattered from a sample. The outgoing beam can be analyzed in terms of the angle, the energy and the inten-

sity.

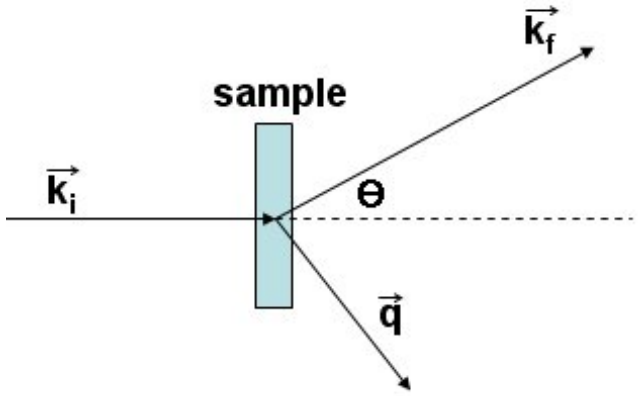

Figure 2: Setup of a scattering experiment.

For the wavevector of the incident beam $\vec{k_i}$, the wavevector of the scattered beam $\vec{k_f}$ and θ being the scattering angle the wavevector transfer $\vec{q}$ can be derived by

$$\vec{q} = \vec{k_f} - \vec{k_i} = \frac{4\pi n}{\lambda} \sin \frac{\theta}{2} \tag{1}$$

where n is the refractive index for the sample. As one can see from the formula a change in q (for a fixed wavelength) is caused by changing the angle.

1.4 Intensity and Scattering Pattern

The intensity can be used to determine Interactions between the particles in the sample.

$$I(q) \sim F(q)^2 * S(q) \tag{2}$$

Where $I(q)$is the absolute square of the so called 'Scattering Amplitude', $F(q)$ is the 'Form factor' and $S(q)$ is the 'Structure factor'.

1.4.1 Formfactor

The Form factor is the Fourier-transform of the scattering particles shape and therefore provides information on their structure.

$$F(q) = \int_V e^{i\vec{q}\vec{r}/\hbar'} \rho(r') d^3 r' \tag{3}$$

For a single electron resting in the origin of our coordinate system the electron-density is descriped by

$$\rho(r') = \int_V e^- * \delta(r') d^3 r' \tag{4}$$

Integrating over the delta function results in $F(q) = 1$ and we gain Rutherford scattering.

With an optical laser we are sensitive to electron density differences in the 10-100 nm-regime. This allows us to analyze the shape of the colloidals. For a homogeneous sperical particle (see fig. 3)[1] $F(q)$ can be derived as

$$F(q)^2 \sim [\frac{\sin(qr) - qr\cos(qr)}{(qr)^3}]^2. \tag{5}$$

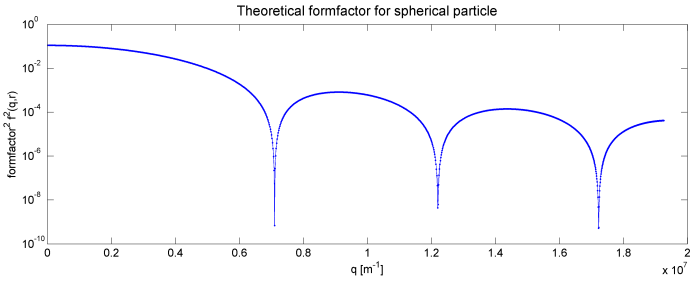

Figure 3: Theoretical form factor for spherical particles with radius 600 nm and λ=633 nm.

1.4.2 Structure factor

Diluted case

For higly diluted samples (no correlations between particles) the structure factor $S(q) = 1$. The colloidal particles move driven by the thermal fluctuations of the solvent and undergo Brownian motion. The mobility of the particles is $\mu = 1/f$, where $f = 6\pi\eta r_H$is the friction coefficient, $r_H$the hydrodynamic radius[2]and η the viscosity of the suspending medium. For highly diluted samples $r_H = r$ is a valid relation.

Using the Stokes-Einstein-Relation $D = \mu k_B T$ we obtain:

$$D_0 = \frac{k_B T}{6\pi\eta r} \tag{6}$$

The other way around, knowing D_0 we can calculate the radius of the solved particles.

[1] As we will see later, this is exactly the pattern we will get for our colloidals

[2] (eq. Stokes Radius) is the radius of a imaginary hard sphere that diffuses with the same velocity as the considered particle

Concentrated solutions

For concentrated systems, where particle-interactions are not neglectable anymore, the structure factor deviates from 1.

A strong interaction would for example cause the particles to form some kind of regularly structure. This would effect a much different scattering pattern, due to the fact that regularly structures create the basic requirement for Bragg-reflection. In this case $S(q)$ will display a maximum at $q_{(Max)}$. This value is related to the mean interparticle spacing[3] via

$$d = \frac{2\pi}{q_{(Max)}} \tag{7}$$

The exact functional form of $S(q)$ will depend on the nature of the interactions described by the interaction potential.

1.5 Photon correlation spectroscopy (PCS) in colloidal dispersions

In addition to (eq.2) the scattered intensity is described by a sum over all (j) scattering particles

$$I(q,t) = |E(q,t)|^2 = [\sum_j a_j(q) e^{i\vec{q}\vec{r_j}(t)}]^2 \tag{8}$$

where a_j is the scattering amplitude, $E(q,t)$ is the superposition of the fields that are instantaneously scattered at the moving particles at the position $\vec{r_j}(t)$. Due to thermic energy colloidal particels perform brownian motion. Measurements of the temporal intensity fluctuations can reveal informations on the underlying dynamics of the sample.

In PCS (as well as XPCS) the measured intensity can be correlated with it's timeshifted identity by a 'digital autocorrelator' to produce the normalized intensity correlationfunction g_2(see figure 4), defined as

$$g_2(q,\tau) = \frac{\langle I(q,0) * I(q,\tau)\rangle}{\langle I(q)^2\rangle} \tag{9}$$

where the brackets $\langle\rangle$ denote an time averaging.
Under the conditions that:

- the spacing volume V contains a large number of particles;
- the spatial correlation range of the particles is much smaller than $V^{1/3}$;
- the particles can diffuse throughout the suspension.;
- the field $E(q,t)$ is a zero-mean complex Gaussian random variable.

[3] Distance between centers of particles

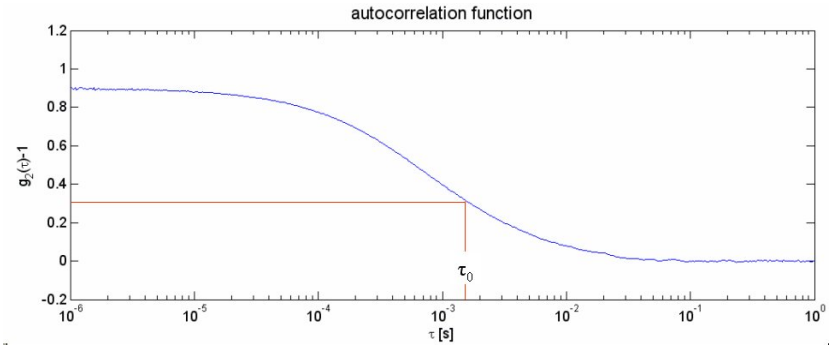

Figure 4: Example for an Intensity-autocorrelation function.

We can express the normalized intensity correlation function $g_2(q,\tau)$ in terms of the normalized intermediate scattering function $f(q,\tau)$ by using the Siegert relation

$$g_2(q,\tau) = 1 + \beta(q^2)\frac{\langle E^*(q,0)\cdot E(q,\tau)\rangle^2}{\langle I(q)\rangle^2} = 1 + \beta(q)[f(q,\tau)]^2 \tag{10}$$

where $\beta(q) = g_2(q,0) - 1$, depends on the coherence properties of the beam. For incoherent radiation, $\beta(q) = 0$ and $g_2(q,\tau) = 1, \forall\tau$. The normalized intermediate scattering function for N identical particles can be written as:

$$f(q,\tau) = \frac{1}{S(q)}\frac{1}{N}\sum_{i=1}^{N}\sum_{j=1}^{N}\langle e^{iq(r_i(0)-r_j(\tau)}\rangle \tag{11}$$

where $S(q)$ is the static structure factor.

In the presence of particle interaction one usually analyzes $f(q,\tau)$ in terms of a cumulant expression

$$f(q,\tau) = e^{-\Gamma_1(q)\tau+\Gamma_2(q)\tau^2-\Gamma_3(q)\tau^3\ldots} \tag{12}$$

where $\Gamma_1(q) = \Gamma(q)$ is the first cumulant. The initial desay of $f(q,\tau)$ describes the effective short-time[4] diffusion coefficient $D(q)$ of the colloidal suspension according to:

$$\lim_{\tau\to 0} -\frac{d\ln f(q,\tau)}{d\tau} = \Gamma(q) = D(q)\cdot q^2. \tag{13}$$

The short-time behavior of the normalized intermediate scattering function $f(q,\tau)$ is

$$f(q,\tau) = e^{-\Gamma(q)\tau} = e^{-D(q)\cdot q^2\cdot\tau.} \tag{14}$$

Thus, from equation (10) and (18) we obtain

[4] the time, which a particle needs to move over a distance about its own size

$$g_s(q,\tau) - 1 \propto e^{-2\Gamma(q)\tau} \tag{15}$$

It can be shown that the short time diffusion coefficient $D(q)$ is given by

$$D(q) = \frac{D_0 \cdot H(q)}{S(q)} \tag{16}$$

where D_0 is the Stokes-Einstein diffusion constant (see eq.6), introducing the contribution from the colloid solvent interaction. The static factor $S(q)$ considers the contribution from direct colloid-colloid interactions, the hydrodynamic function $H(q)$ describes indirect particle interactions, mediated by the fluid.

1.6 Temperature dependence of viscosity

During our experiment we want to determine motion and interaction of solved particles. Therefore we have to consider the change in viscosity of water that comes along with different temperatures. According to a paper by 'Preston M. Kampmeyer'[5] the viscosity of water can be described by

$$\eta(T) = a \cdot \exp(b + c * (T/1000) + d * (T/1000)^2 + e * (T/1000)^3), \tag{17}$$

where η is the viscosity and T the temperature in Kelvin. a,b,c,d and e are fitting parameters we can find by performing a χ^2 minimization-Fit, using a dataset found on the internet.

[5] Journal of Applied Physics, Vol 23, Number 1, January 1952 - "The Temperature Dependence of Viscosity for Water and Mercury"

2 Experiment

2.1 Experimental setup

The light source is a 633nm HeNe-Laser. In most of the cases it is necessary to decrease the laser-intensity. For that purpose there are two wheels with distinct absorbers which the laser has to pass. For later calibration the beam is splitted and the intensity is measured by a diode. Now the beam is focused into the sample and diffracted. By using a detector that is mounted onto a goniometer we can analyze the scattering pattern within a range of $\theta = 30°$ to $\theta = 150°$. Since we need a very high time-resolution ($<10^{-6}$sec) we are using a hardware autocorrelator that works with a time resolution of 15 ns. Software-based analysis would be far to slow for our purpose.
The sample is mounted into a temperature-chamber. A chiller is used to define the temperature in the chamber a range of roughly 5° to 60° C. The aberration from the setpoint of temperature increases with temperature. At 50°C we measure an aberration from setpoint to real temperature of about 1,5°C via a calibrated thermometer.

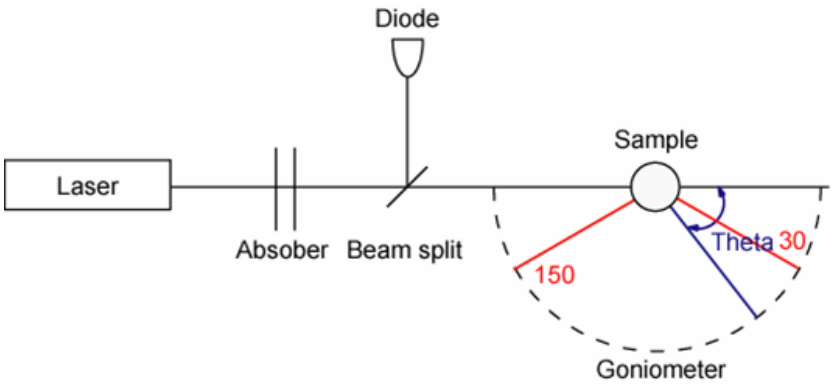

Figure 5: Picture of the experiment

2.2 Viscosity correction

We use a dataset found on the internet [6] to calculate the viscosity correction. We obtain the following parameters and thus we reach a very good interpolation of the dataset (see fig. 6).

$a = 18.7mpas \cdot s, b = -106.1, c = 154.2K^{-1}, d = -35.5K^{-2}, e = 1K^{-3}$

[6] http://www.thermexcel.com/english/tables/eau_atm.htm

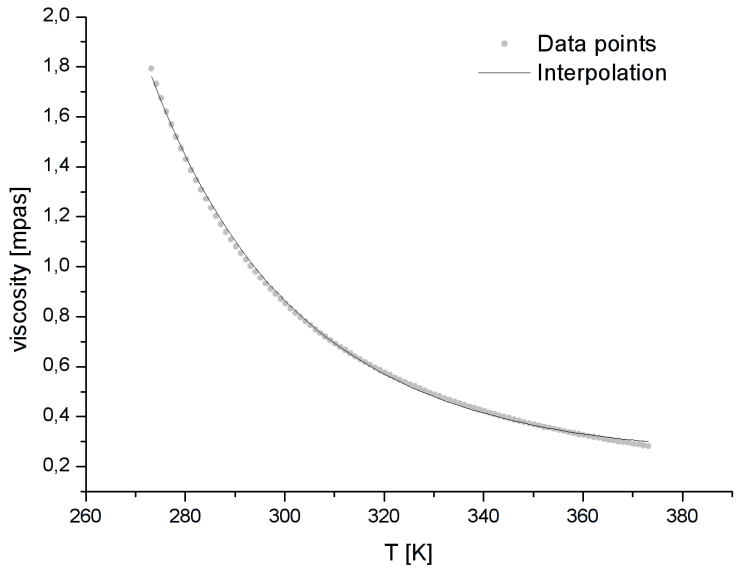

Figure 6: Temperature dependence of viscosity of liquid water

2.3 Temperature correction

As mentioned before the temperature measured at the chiller is not equal to the temperature in the sample holder. This has different reasons. The two most contributing factors are the relatively long and not isolated hoses that lead from the chiller to the sample-holder and the sample-holder itself. It's made of metal and due to a metals very good heat-conductivity there is a continuously heat-loss that is proportional to the temperature difference between the inside and the outside of the chamber. The room-temperature is regulated to about 23°C.

Up from now mentioning of temperature will always refer to the ones measured at the sample position.

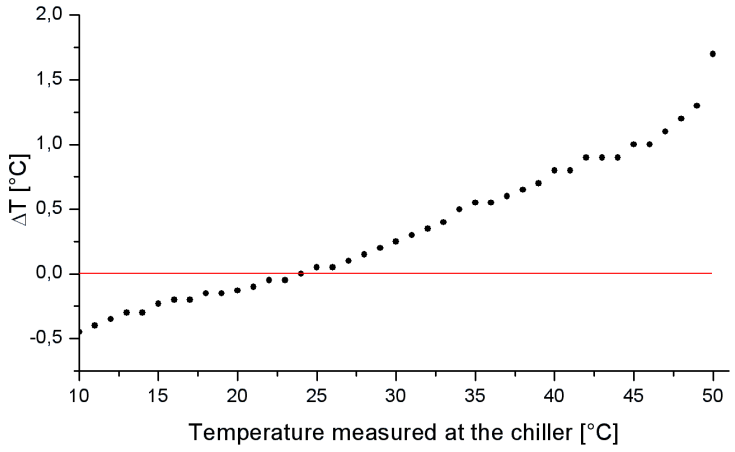

Figure 7: Difference between measured temperatures at the chiller and the sample holder

3 PMMA

3.1 PMMA diluted sample

The PMMA particles we are analyzing are solved in water and predicted to have a size of about 60n m. We take a series of autocorrelation functions from θ= 40° to θ=150° in 1° steps. The following procedure was automatized by a MatLab-Program in order to determine some characteristics of the sample, such as the 'particle radius', the 'diffusion constant' and the 'hydrodynamic function'.

3.1.1 Autocorrelation function

As mentioned before for a diluted sample we can use an exponential decay, see equation (15), to describe the behavior of the autocorrelation function very well. Γ is our fitting parameter and for this sample we get figure (8). Obviously the fit is a very good interpolation for the measured data.

3.1.2 Diffusion constant

According to equation (13) Γ shows a quadratic dependence on q, where this time D_0 is the fitting parameter for our fit.

Obviously the q^2-dependency is not perfectly fulfilled (see figure 10). The most reasonable explanation is, that the particle interaction is not totaly neglectable due to a insufficient dilution.

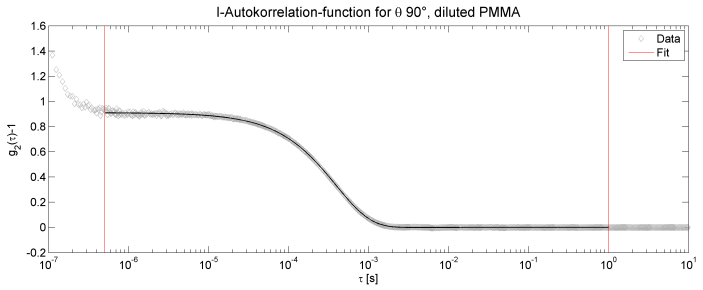

Figure 8: Autocorrelation function for diluted PMMA, $\Gamma = 1274s^{-1}$

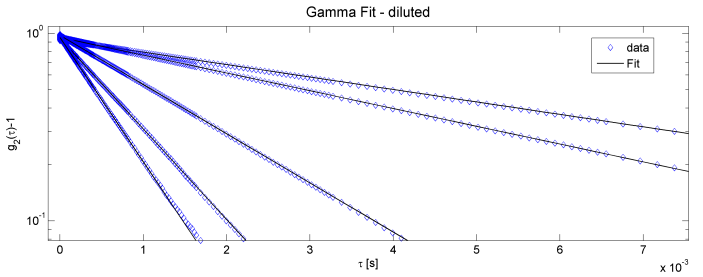

Figure 9: Logscale presentation of Γ-Fit for conditions equal to figure (8) for 5 q-values ($q = 1, 1.4, 1.8, 2.2, 2.6 * 10^7 m^{-1}$)

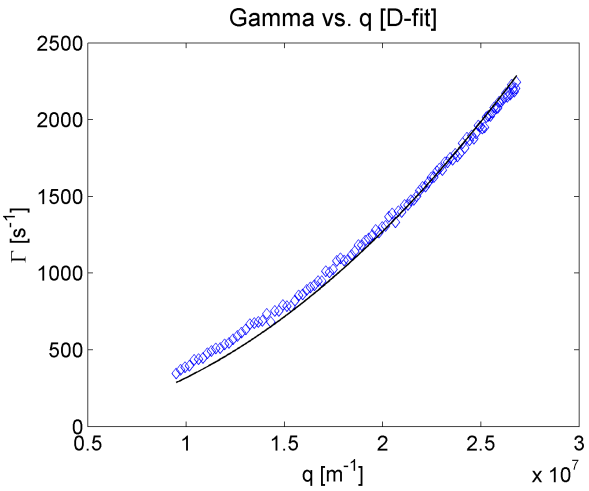

Figure 10: q^2 dependence of Γ in diluted case PMMA. The solid line represents $\Gamma = q^2$.

3.1.3 Determination of radius

From equation (6) we can calculate the radius of our particles to **66.9 nm** $\pm$**5nm**. This is very close to the predicted radius of 60 nm. Thus we can say,

that this method seems to deliver satisfying results.

3.1.4 Intensity and Form factor

With knowledge about the particles radius it's possible to calculate the theoretical formfactor of our particles after eq.(5). According to equation (2) for diluted samples, $S = 1$, the scattered intensity should show the same behavior as the formfactor squared, if plotted against q. This is done in figure 11

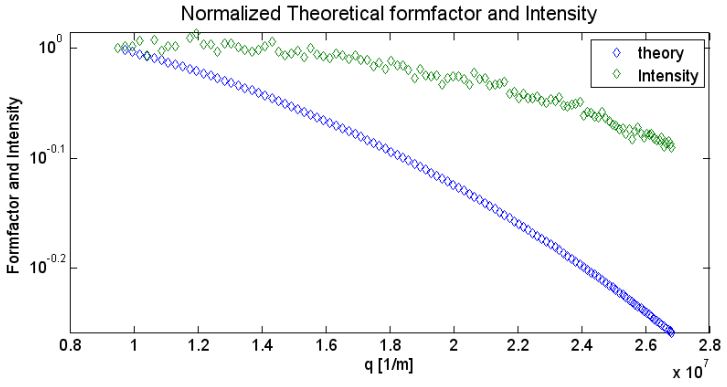

Figure 11: Theoretical form factor for a spherical particle of size r=66 nm compared with the real measured intensity.

Obviously this is not the case in our sample. The theoretical prediction and the measured intensity have the same shape, but differ in their slope. Reasons could be a insufficient dilution and the according interparticle correlation.

3.2 PMMA concentrated sample

This time we analyze the same sample as before but in a higher concentrated version, so we can directly compare diluted and concentrated samples and figure out the effects the increasing interactions have on the scattering behavior. As one can see the relation given by equation (13) is not valid anymore. For small q-values there is a strong deviation from the ideal q^2 trend (see fig. 13)

3.2.1 Intensity

In comparison with the intensity for the diluted sample there is a clear peak at $q = 1.4 \cdot 10^7 m^{-1}$ in the concentrated one (see fig.(14)). This peak is due to interparticle correlations.

3.2.2 Static structure factor

The static structure factor S(q) is extracted from the data by dividing the measured intensity I(q) for the concentrated sample by the measured intensity

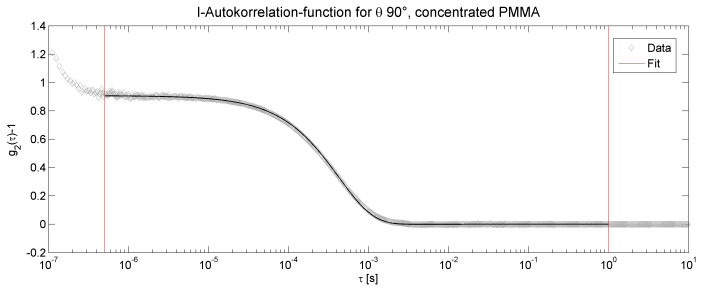

Figure 12: Autocorrelation function for concentrated PMMA, $\Gamma = 1274s^{-1}$

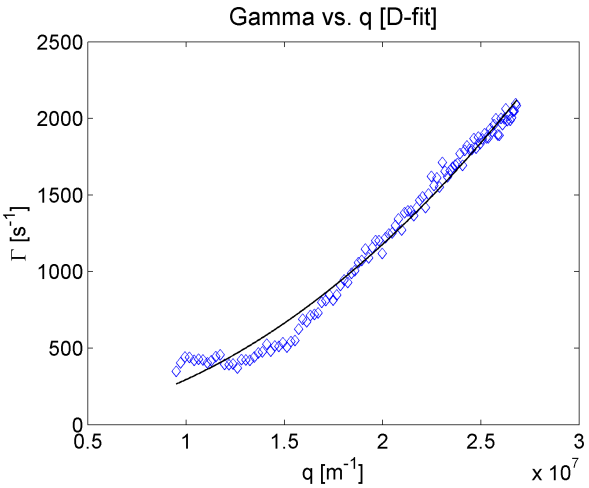

Figure 13: q^2 dependence of Γ in concentrated case PMMA. The solid line represents $\Gamma = q^2$.

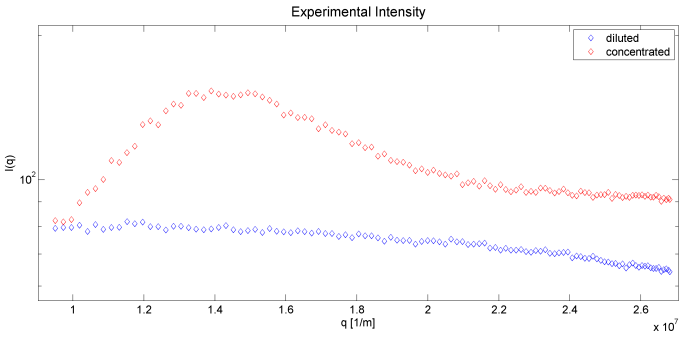

Figure 14: Static intensity for diluted and concentrated PMMA sample

for the diluted sample. $S(q) = \frac{I(q)_{conc}}{I(q)_{dil}}$. The resulting structure factor is shown in figure 15(a). The peak position of the static structure factor $q_{max} = 1,4 \cdot 10^7 m^{-1}$ is related to the mean interparticle spacing d by $d \approx \frac{2\pi}{q_{max}}$ (see eq. 7). The calculated mean interparticle spacing is roughly 450 nm. As we know for the diluted case (eq. 13) is a valid relation. However the concentrated case can not be treated with the diluted theory. $D(q)$ is considerably smaller, than D_0 and not longer a constant in q. In order to quantify the deviation from the diluted case the ratio $D_0/D(q)$ is computed and displayed in figure 15(b) and compared with the static structure factor $S(q)$. The behavior of the normalized inverse diffusion coefficient $D_0/D(q)$ mimics the behavior of $S(q)$. In ideal case there is a pronounced maximum in this case indicating that the dynamics is slowed down and reaches a minimum for wavevector transfers corresponding to the peak of the structure factor. This effect is most pronounced for the higher concentrations. Any deviations of $D_0/D(q)$ from the static structure factor $S(Q)$ is an indication for the presence of indirect, hydrodynamic interactions. As you can see in figure 15(d) there are deviations of the normalized inverse diffusion coefficient $D_0/D(q)$ from the static structure factor $S(Q)$ for the whole q-range. This clearly shows that hydrodynamic interactions are present and influence the dynamics.

3.2.3 Hydrodynamic interactions

The hydrodynamic behavior of the studied system can be quantified in the short-time limit, by rewrite the hydrodynamic functions $H(q)$, using eq.(16) to obtain

$$H(q) = S(q) \cdot \frac{D(q)}{D_0} \tag{18}$$

Figure 15(c) shows the hydrodynamic function $H(q)$ for the PMMA concentrated sample. As can be seen, $H(q) < 1$ for all wavevector transfers q, thus showing that the hydrodynamic effects play role of an additional friction force.

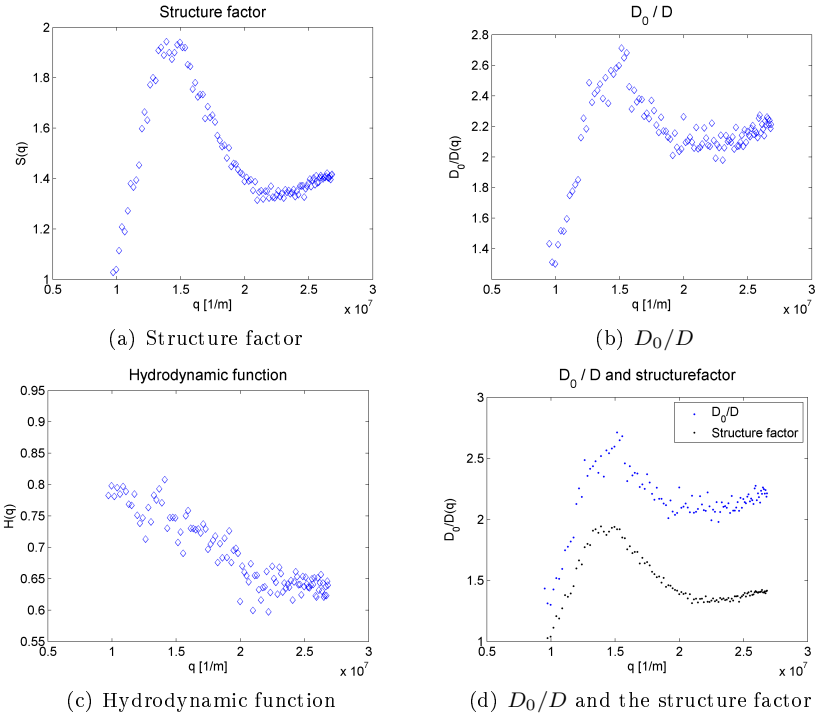

(a) Structure factor (b) D_0/D

(c) Hydrodynamic function (d) D_0/D and the structure factor

Figure 15:

4 pNIPA - in 3 concentrations

- pNIPA 1by1 - is a concentrated sample, prepared by mixing 50 % vol. poly-NIPA particles and 50 % vol. distilled water.
- pNIPA 1by8 - is a sample, prepared by mixing 20 % vol. poly-NIPA particles and 80 %vol. distilled water.
- pNIPA 1by100 - is our diluted sample. It consists of 1 part pNIPA-particles dispersed in 100 parts distilled water.

4.1 Static Analysis

During analyzing the data it became obvious that the most interesting processes happened in at temperatures of about 20°C. For our samples this was the critical temperature region for the glass transition to happen. The transfer into glassy phase is accompanied by a complete change in the dynamic, as well as in the static behavior.

1by1-sample

With decreasing temperature our 1by1 sample became more and more opaque. The absorbtion for visible light became too strong, to obtain any useful static data. For small scattering angles the laser beam has to pass a much longer distance within the sample (see fig. 16), due to that more absorbtion occurs and the scattering pattern goes under in the comparable strong effect of absorbtion.

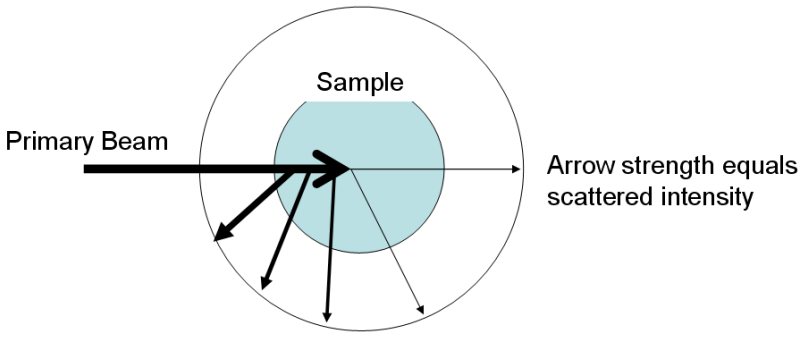

Figure 16: Absorption in sample has influence on the scattered intensity.

1by8-sample

Absorbtion comes into account in the 1by8 sample too, but its effect is weak compared to the one the structure factor has. As can be seen in figure 17 the scattered intensities are very different for the high and low temperature. This can be explained by the growing of the particles, accompanied by a self ordering, resulting in a partially regularly structure that causes Bragg-peaks in the measured intensities.

4.2 Particle radius

As before for PMMA we determine the radii of our particles in the solution via Γ-Fit $\rightarrow$ D_0-Fit $\rightarrow$equation(6). We obtain a curve of radius vs. temperature which is very similar to known literature. This method is obvious very sensitive to effects caused by insufficient dilution. Figure 18 demonstrates that, for the 1by8 sample we gain radii that are a factor 1.5 to 2 bigger than in the diluted case. For the 1by1-sample we do not even try to determine the radius because several effects come into account we want to discuss now.

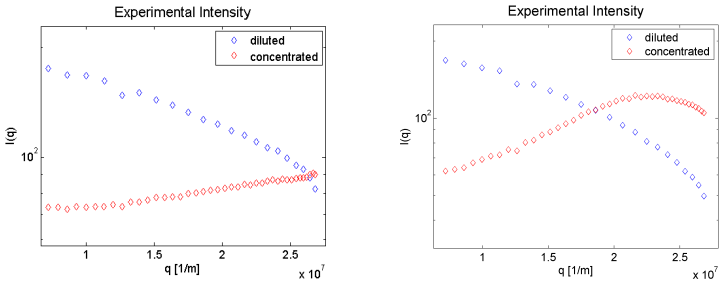

(a) Scattered intensity for 28° - Absorbtion takes effect, intensity is decreased for small angles.

(b) Scattered Intensity for 15° - Structure factor causes a peak due to the ordering in the system.

Figure 17: Scattered Intensity for 1by8 and 1by100-sample at temperature 15°C and 28°C.

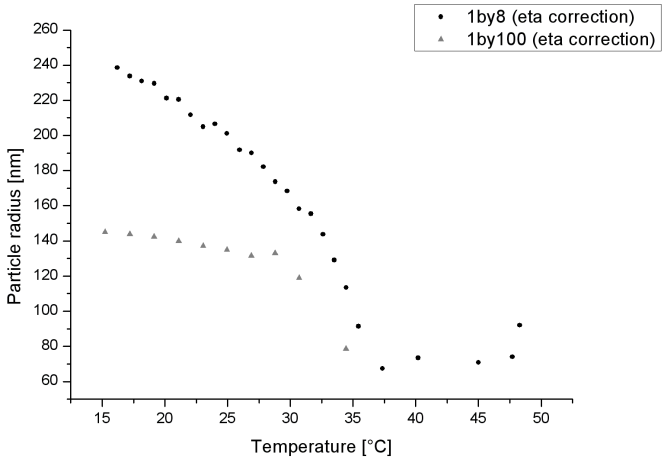

Figure 18: Temperature dependence of radius

4.3 Discussion of dynamic behavior (1)

At about 20°C and below we could notice strong changes in the dynamic behavior of our 1by1-sample. The exponential decay does not describe the autocorrelationfunction correctly anymore, as can be seen from figure 19. For high temperatures (Fig.19(a)) there is a noticeable deviation from the exponential decay (see eq.15). However for temperatures far below the glass transition temperature, in our case 10°C the autocorrelation function can not be described by an exponential decay at all (see figure 19(c)).
Some Authors discuss the possibility to describe the behavior of the autocorrelation function by a 'Stretched exponential decay', such as

$$g_s(q,\tau) - 1 \propto e^{-2\Gamma(q)\tau^b} \tag{19}$$

Indeed this leads to a much better fit for high temperatures, as can be seen in figure 19(b).

4.4 Discussion of dynamic behavior (2)

As mentioned before a phase-transition can not only be reached by temperature change, but also by changing the concentration of particles within a system. Figure 20 demonstrates this in a very convincing way. For the 1by100-sample the exponential decay works very well. With increasing concentration the fit describes the curve less good and finally for the 1by1-sample not at all. An offset is visible, that is due to no more moving, crystalized areas in the sample.

The reason why this offset was not visible in figure 19(c) at an even lower temperature is due to the experimental procedure. The measurements for 20(c) have been taken separately, with a fast decrease of temperature from 35° to 15°C. In contrast to that the measurement for figure 20(c) was part of a series of measurements with a very slow, stepwise decrease of temperature from 30° to 15°C. This can (and obvious has) influence on the crystallization behavior of our sample. Because our setup is probing only a very small part of the sample there is another aspect, why the two measurements differ. The process of crystallization happens randomly. Therefor orientation, size and place of the crystalized areas are unpredictable and results not exactly reproducible.

4.5 Discussion of dynamic behavior (3)

Now we want to have a closer look at the temperature dependent behavior of the autocorrelation functions for our 1by1-sample. In figure 21 we have plotted the normalized autocorrelation functions for temperatures from 11° to 28°C for the 1by1-sample. We splitted the temperature range into two plots because there is a very significant change in behavior towards 20°C.
In figure 21(a) the temperatures higher than 20°C are plotted and the autocorrelation functions arrange in a very ordered way. With decreasing temperature τ_0 becomes bigger, what means the system slows down.
Figure 21(b) contains the autocorrelation functions for temperatures below the glass transition temperature. In contrast to the first plot there is no system or order in which the autocorrelation functions arrange.

The fact that something radically changes is also reflected in figure 22. For this figure we extracted different values, namely:

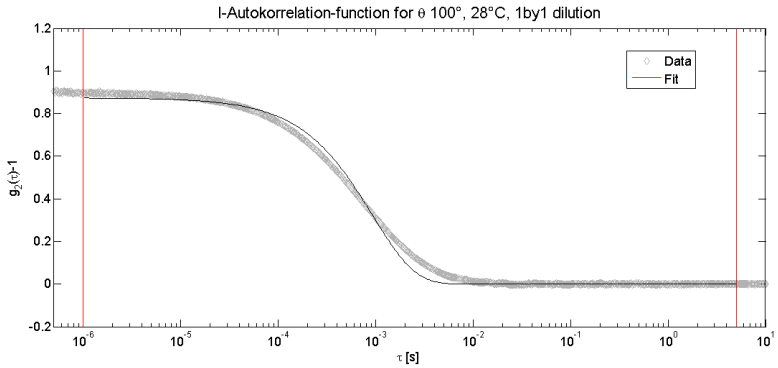

(a) Autocorrelation function at 28°C, exponential decay, $\Gamma = 166s^{-1}$

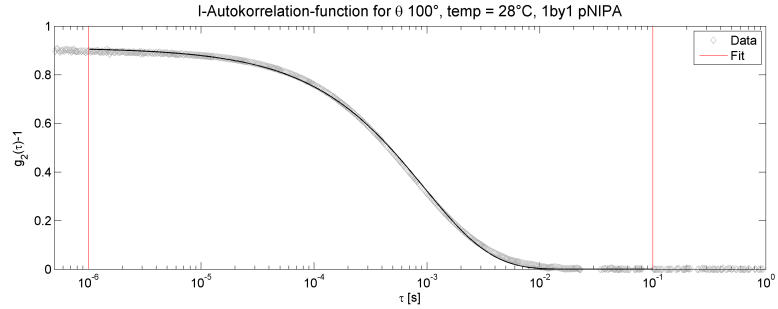

(b) Autocorrelation function at 28° C, stretched exponent fit, $\Gamma = 80s^{-1}, b = 0,73$

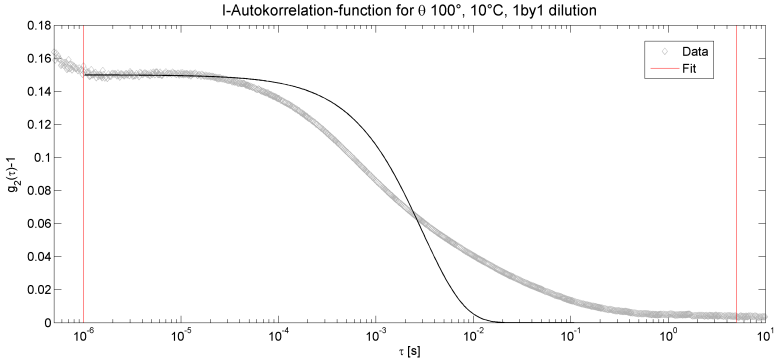

(c) Autocorrelation function at 10° C, exponential decay, $\Gamma = 536s^{-1}$

Figure 19: Autocorrelation function for pNIPA 1by1-sample

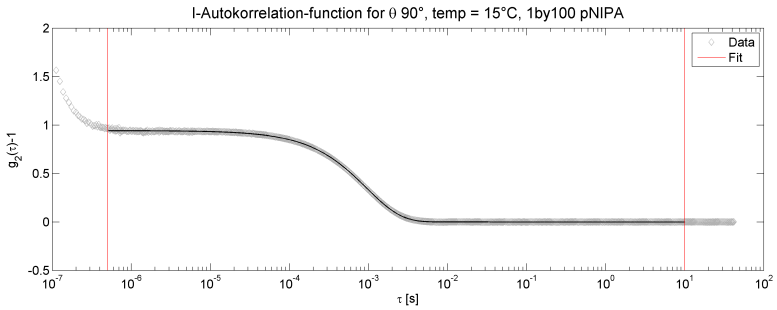

(a) Autocorrelation function for 1by100 dilution, $\Gamma = 522s^{-1}$

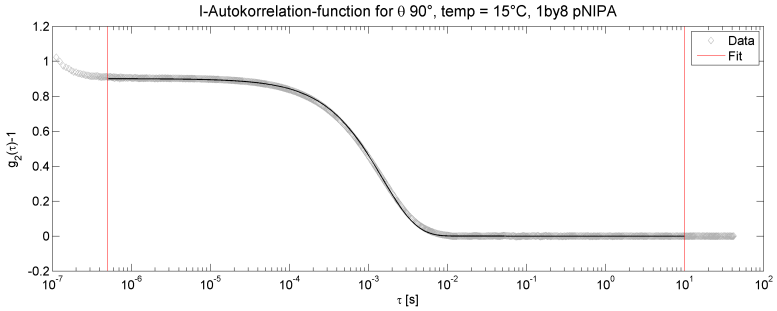

(b) Autocorrelation function for 1by8 dilution, $\Gamma = 334s^{-1}$

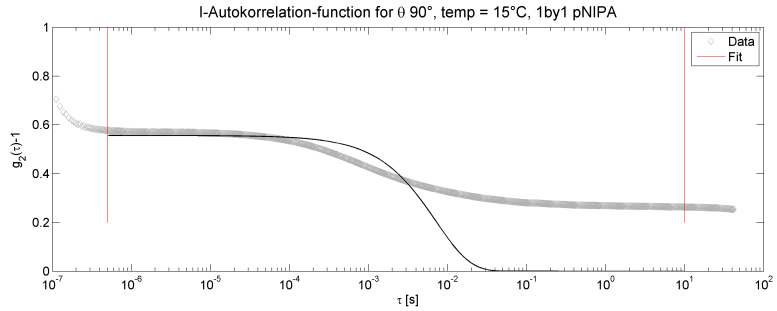

(c) Autocorrelation function for 1by1 dilution, no fit possible, $\Gamma = 70s^{-1}$

Figure 20: Autocorrelation functions for pNIPA at T=15°C

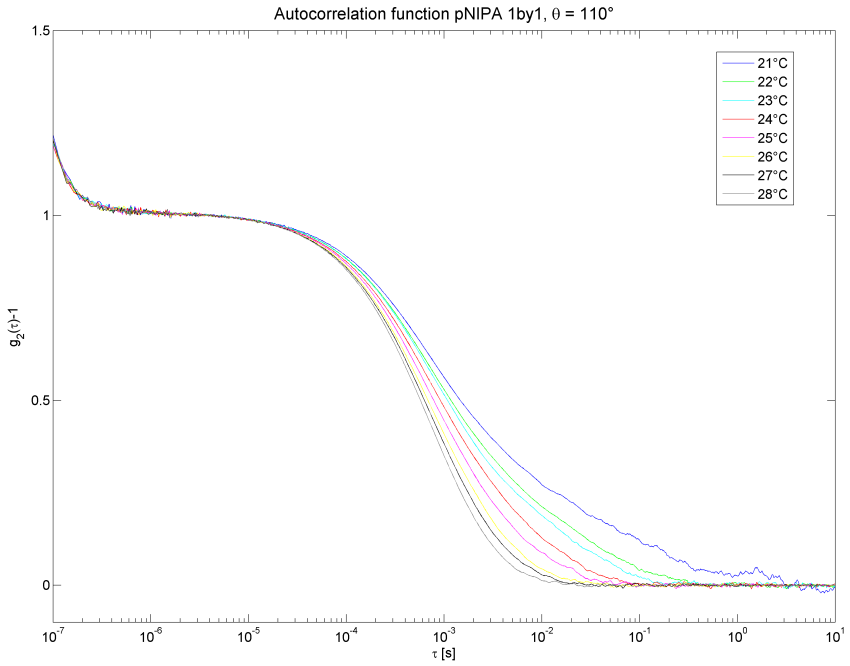

(a) Autocorrelation function for the temperatures above 20°C.

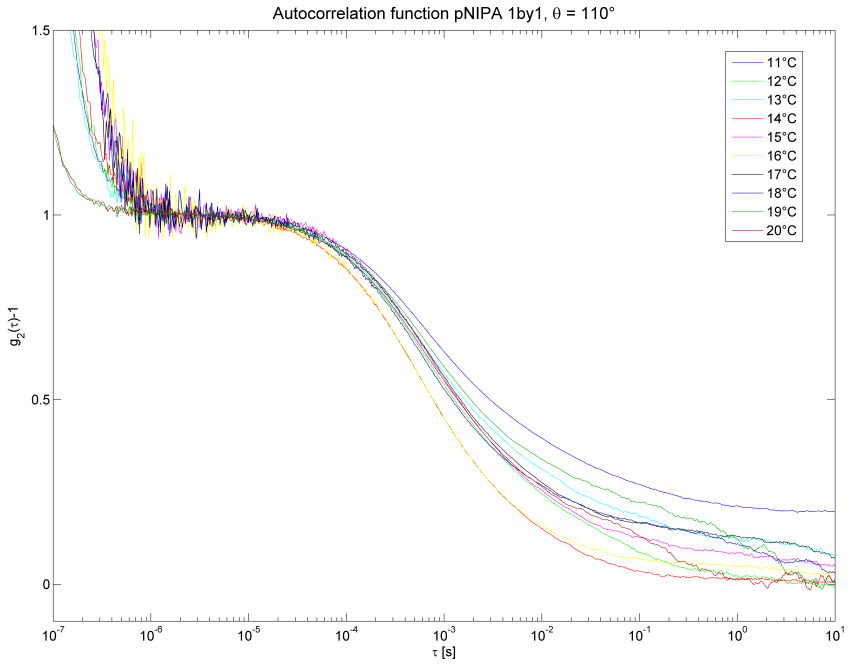

(b) Autocorrelation functions for temperatures below 20°C.

Figure 21: Autocorrelation functions for 1by1 dilution.

- The 'offset' is the value of the lower plateau of the autocorrelationfunction. A value $\neq 1$ means there are "frozen", not moving areas in the analyzed part of the sample.
- The 'contrast' is the difference between the upper and lower plateau in the autocorrelation function.
- The 'Γ-value', is extracted from the autocorrelation functions by a fit of equation 15 for the short time behavior of the sample.
- 'exponent stretch' is the b-value from equation 19.
- 'R^2' - is a measure of how good the fit agrees with the measurement. In the case perfect extrapolation R^2=1.

All the plots from figure 22 have one thing in common. For high temperatures ($T > 20°C$) the data points show a very ordered behavior. However for temperatures ($T < 20°C$) the data points scatter chaotically. This is certainly due to a phase change from the liquid to the glassy state.

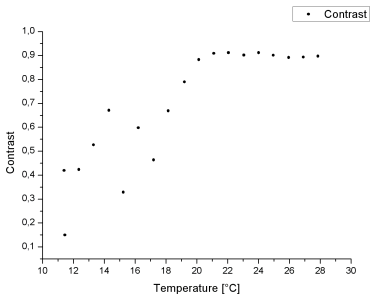

(a) Contrast vs. temperature

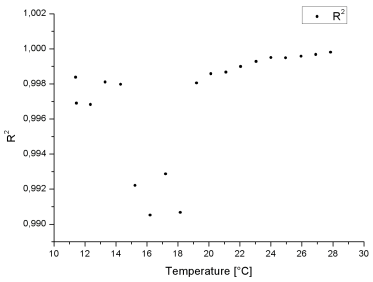

(b) R^2 vs. temperature

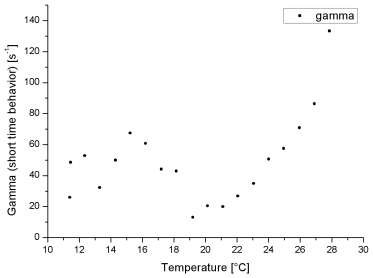

(c) Γ for short time behavior vs. temperature

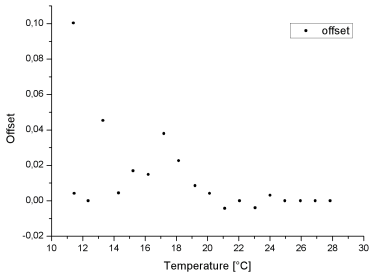

(d) Offset vs. temperature

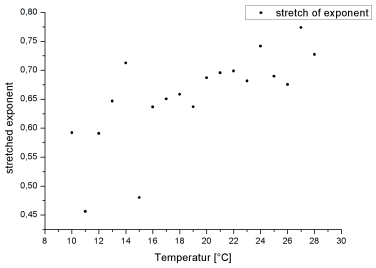

(e) Stretched exponent vs. temperature

Figure 22: Analysis of 1by1 autocorrelation functions

5 Conclusion

In this work we performed DLS experiments on colloidal systems, namely PMMA and pNIPA particles in a aqueous solution. The size of the pNIPA particles shows a very high dependence on the temperature and thus we can change the system between liquid and glassy phase by controlling the temperature. We measured the static intensity and the intensity-autocorrelation function in order to obtain information about the static and dynamic processes within our samples. As a result we can say, that for high dilutions we have a very good correspondence between the dynamic theory respecting Brownian motion and our measurements (exponential decay in autocorrelation function). This correspondence gets lost for the highly concentrated 1by1 and even for the 1by8 sample when we go to low temperatures. A strong influence of the structure factor is observable. The loss of correspondence as well as the contribution of the structure factor lead to the conclusion that the pNIPA 1by1 and 1by8-sample perform a change from the liquid to the glassy state. In this state the theory describes the dynamic behavior of our particles very insufficient. However the diluted theory can be modified by using a 'stretched exponential decay' for temperatures close below the glass transition temperature and still make good predictions for the dynamic behavior.